This article has been accepted for inclusion in a future issue of this journal. Content is final as presented, with the exception of pagination.

Variable Time Headway Policy Based Platoon Control for Heterogeneous Connected Vehicles With External Disturbances

Yongfu Li, *Senior Member, IEEE*, Qingxiu Lv, Hao Zhu, *Member, IEEE*, Haiqing Li, *Associate Member, IEEE*, Huaqing Li, *Senior Member, IEEE*, Simon Hu, *Member, IEEE*, Shuyou Yu, *Member, IEEE*, and Yibing Wang, *Member, IEEE*

***Abstract*— This article develops a new platoon control strategy for heterogeneous connected vehicles (CVs) subject to time delays and external disturbances. Specifically, based on the third-order vehicle model, a novel platoon controller is developed by embedding the variable time headway (VTH) spacing policy and the nonlinear motion coupling interactions between CVs. Simultaneously, an integral sliding mode (ISM) controller is developed to resist the disturbances. Then, the condition of asymptotic stability for the CV platoon and the upper bound of communication delay are deduced by using the Lyapunov theorem. Also, the string stability is proved by using the infinity-norm method. Finally, extensive simulations and co-simulations are provided to show the validity of the developed controller. Moreover, experiments with intelligent micro vehicles are conducted further to validate the practical feasibility of the developed controller.**

***Index Terms*— Connected vehicle, platoon control, spacing policy, motion coupling interactions, disturbances.**

I. Introduction

A. Motivation

PLATOON-BASED driving has recently received widespread attention due to the booming growth of connected vehicle (CV) technologies [1]–[3]. By taking advantage of advanced wireless devices, state information can be easily shared between CVs. Further, through the platoon controller, CVs in a string can reach consensus and form a stable formation. That is, all CVs run on the way at the same velocity and desired inter-vehicle gap, thus greatly enhancing traffic efficiency and reducing adverse environmental impacts, etc. Despite the extensive research and significant progress in this field, there are still unresolved difficulties, which can be summarized as the subsequent aspects. Firstly, the spacing policy is important for the platoon control as it will determine the rationality of the pre-set inter-vehicle gap and further affect the traffic safety and road capacity accordingly. While the two traditionally spacing policies, namely constant time headway (CTH) policy, and constant spacing (CS) policy, are not flexible enough, especially for the rapidly changing velocity situation, at the cost of low traffic flow and vehicle collisions. Consequently, it is an urgent task to employ a more effective spacing policy. Secondly, vehicles in the platoon are not single individuals, and there are motion coupling interactions between them. Ignoring the interactions may result in the mismatch between vehicle behavior and traffic flow theory (e.g., negative velocity and unreasonable acceleration). Thirdly, time delays caused by unreliable communication, as well as the external disturbances suffered from complex environments, should be properly tackled. Otherwise, it may lead to performance deterioration and instability of the platoon and even make the platoon break up.

Although one or two of the above issues has been considered in literature, rarely all of them have been taken into account. How to design a more efficient platoon controller in this context is meaningful. To this aim, this article attempts to develop a new variable time headway (VTH) policy based platoon controller by considering motion coupling interactions so as to eliminate the adverse impacts of external disturbances and time delays.

B. Related Work

There has been a lot of research on the consensus-based control methods for CV platoon [4]–[18]. According to whether all vehicles in the platoon share an identical vehicle model, we can basically classify the consensus-based control schemes into homogeneous model-based methods and heterogeneous model-based methods.

1) Homogeneous Vehicle Model-Based Methods: Homogeneous vehicle models mainly include the first- and second-order integrator models. Considering that the first-order model

Manuscript received September 1, 2021; revised December 25, 2021 and February 24, 2022; accepted April 22, 2022. This work was supported in part by the National Natural Science Foundation of China under Grant U1964202, Grant 61773082, and Grant 62073052. The Associate Editor for this article was K. C. Leung. *(Corresponding author: Yongfu Li.)*

Yongfu Li, Qingxiu Lv, Hao Zhu, and Haiqing Li are with the Key Laboratory of Intelligent Air-Ground Cooperative Control for Universities in Chongqing, College of Automation, Chongqing University of Posts and Telecommunications, Chongqing 400065, China, and also with the Zhejiang Laboratory, Hangzhou 311121, China (e-mail: liyongfu@ieee.org).

Huaqing Li is with the College of Electronic and Information Engineering, Southwest University, Chongqing 400715, China (e-mail: huaqingli@swu.edu.cn).

Simon Hu is with the School of Civil Engineering, Zhejiang University/University of Illinois at Urbana-Champaign Institute, Zhejiang University, Hangzhou 310058, China (e-mail: simonhu@zju.edu.cn).

Shuyou Yu is with the Department of Control Science and Engineering, Jilin University, Changchun 130012, China (e-mail: shuyou@jlu.edu.cn).

Yibing Wang is with the College of Civil Engineering and Architecture, Zhejiang University, Hangzhou 310058, China (e-mail: wangyibing@zju.edu.cn).

Digital Object Identifier 10.1109/TITS.2022.3170647

1558-0016 © 2022 IEEE. Personal use is permitted, but republication/redistribution requires IEEE permission.
See https://www.ieee.org/publications/rights/index.html for more information.

Authorized licensed use limited to: Zhejiang Lab. Downloaded on May 06,2022 at 00:50:41 UTC from IEEE Xplore. Restrictions apply.

This article has been accepted for inclusion in a future issue of this journal. Content is final as presented, with the exception of pagination.

is too simple to accurately describe the vehicle behavior and it is rarely used at present, we mainly discuss the second-order model-based control methods. Reference [4] proposed a second-order distributed controller for platoon with heterogeneous time delay. Reference [5] designed lateral and longitudinal controllers for the multiple platoons and single platoon, respectively. Reference [6] investigated the VTH policy-based platoon controller under switching topology. Reference [7] developed a controller to investigate the influence of communication abnormality on the vehicle platoon. Reference [8] designed a controller to handle the platoon instability when the topology and control gains are changed. However, the nonlinear motion interactions between vehicles that are crucial to transportation engineering are neglected in [4]–[8], which implies that the possibility of negative speed and unreasonable acceleration, as well as the potential risk of vehicle collisions, have not been appropriately resolved. Recently, [9] designed a controller based on dynamic gain to tackle the issue of vehicle collision avoidance, but the phenomenon of acceleration amplitude rapid oscillation still exists. References [10] and [11] developed the controller by considering nonlinear motion coupling interactions between CVs, and showed that negative velocity and unreasonable acceleration rate are well avoided.

2) Heterogeneous Vehicle Model-Based Methods: To better describe some characteristics of the vehicle, such as vehicle heterogeneity and inertia delay in vehicle powertrain system, the third-order model is widely used. Reference [12] developed a controller that factors velocity constraints based on the third-order model under two different topologies. Reference [13] developed a linear controller for the platoon with bounded parametric uncertainty. Reference [14] proposed a distributed PID controller to handle the platoon in view of both homogeneous time delays and time-varying model uncertainty. Reference [15] designed a third-order controller incorporating the acceleration of the leading vehicle and suggested that the acceleration can improve the tracking accuracy. Similarly, in [16], a feedforward-feedback controller considering the acceleration of the front vehicle was designed based on PF topology. It concluded that the responsiveness of the platoon is significantly improved. Reference [17] proposed a third-order platoon controller by considering the packet drop, time delays and the acceleration difference. Reference [18] proposed a third-order CTH policy based platoon controller with heterogeneous delay. Nevertheless, the nonlinear motion coupling interactions between vehicles are not considered in [12]–[18], resulting in unreasonable acceleration.

In addition, it is noted that two problems lie in the above works. One is that they assume that the driving scene of the vehicle is under ideal conditions, so the impact of external disturbances on the performance of CV platoon was ignored. The other one is that the rationality and applicability of the spacing policy are not considered. In fact, due to the uncertainty, vehicles will inevitably be affected by external disturbances, which may lead to the amplification of spacing errors along platoon, causing platoon string instability [19]–[21]. Therefore, necessary measures should be taken to deal with the impact of external disturbances on the platoon. In addition, works in [22]–[25] have also studied the impact of different spacing policies on vehicle platoon performance. They suggest that although CS and CTH policies are commonly used in existing works, however, these policies are implicitly adopted under the supposition that the platoon always tracks a constant desired velocity, which is not practical and applicable for complex driving conditions. On the contrary, the variable reference velocity is more desirable and general, but it may lead to ungratified platoon behavior under these two policies [24] and [25]. Recently, [6] introduced a new VTH spacing policy, which can timely adjust the desired inter-vehicle gap for changing reference velocity. It is verified that the VTH policy has better applicability and potential to improve road capacity and safety. However, there are little works on platoon control based on VTH policy. Hence, the VTH policy is adopted in this article.

C. Contribution

To ensure the tracing performance of vehicle platoon under the circumstance of changing reference velocity and external disturbances, we develop a novel CV platoon controller, and the main contributions are as following threefold:

(i) A more practical third-order VTH-based platoon controller is proposed by considering nonlinear motion coupling interactions and time delays as well as external disturbances. By doing so, the desired inter-vehicle gap can be dynamically adjusted, rather than a fixed value. Therefore, the problems of inflexible spacing adjustment and low road utilization are effectively tackled. Furthermore, the disturbance rejection and the smoothness of the platoon are significantly improved.

(ii) The asymptotic stability and string stability of the CV platoon are rigorously proved by utilizing the Lyapunov-Krasovskii method and infinity-norm method, respectively. Hence, the stablility and the attenuation of spacing error along the platoon are simultaneously guaranteed.

(iii) Different from [3]–[6], [9]–[11], [14], and [17], not only numerical simulations, but also co-simulations in MATLAB/Simulink and PreScan are performed to verify the effectiveness. More importantly, experiments with intelligent micro vehicles (IMVs) are also conducted to testify the practical feasibility of the developed platoon controller.

D. Organization

The structure of the article is as follows: Section II gives the problem statement and preliminary. Section III develops the controller and performs convergence and string stability analysis. Section IV presents the simulation results. Section V shows the co-simulation results. Section VI provides the experimental results. The last section provides conclusions.

II. Preliminaries and Problem Statement

A. Graph Theory

Fig. 1 presents the specific CVs platoon scenario consisting of one leader (noted as $i = 0$) and N followers (noted as $i = 1, \ldots, N$) traveling on a straight road. In this article,

Authorized licensed use limited to: Zhejiang Lab. Downloaded on May 06,2022 at 00:50:41 UTC from IEEE Xplore. Restrictions apply.

This article has been accepted for inclusion in a future issue of this journal. Content is final as presented, with the exception of pagination.

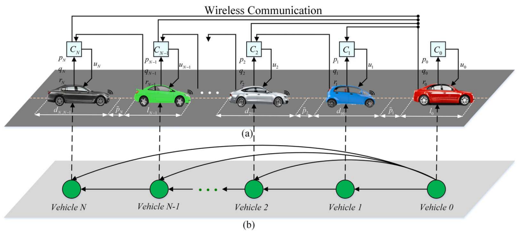

Fig. 1. Platoon control scheme: (a) CV platoon; (b) PLF topology.

we use the predecessor-leader following (PLF) topology to represent the information interactions between CVs.

The graph $V = \{G, A, K\}$ is used to specify the information topology, where $G = \{1, 2, \dots, N\}$ and $A \subseteq G \times G$ are the set of nodes and edges respectively. $K = [k_{ij}]_{N\times N}$ is the adjacency matrix used to describe the connections between CVs, and $k_{ij} = 1$ if $(i, j) \in A$; otherwise, $k_{ij} = 0$. Also, the pinning matrix $B = \mathrm{diag}(k_{10}, k_{20,} \dots, k_{N0})$ is defined to depict the information link between followers and the leader. If there is an information interconnection between the leader and follower i, then $k_{i0} = 1$; otherwise, $k_{i0} = 0$.

B. Mathematical Preliminaries

Now, we give some helpful Lemmas as follows.

Lemma 1 ([26]): Suppose there is a polynomial with complex coefficients:

$$\begin{aligned} r(s) = s^3 &+ (\mathrm{Re}(c_1) + \mathrm{i}\,\mathrm{Im}(c_1))s^2 + (\mathrm{Re}(c_2) \\ &+ \mathrm{i}\,\mathrm{Im}(c_2))s + (\mathrm{Re}(c_3) + \mathrm{i}\,\mathrm{Im}(c_3)) \end{aligned} \tag{1}$$

where $c_1, c_2, c_3 \in C$, $r(s)$ is Hurwitz stable if and only if the corresponding principal minor for (1) are positive.

Lemma 2 ([27]): If $f : [x, y] \to R$ is a convex function, the following result holds:

$$f(\frac{x+y}{2}) \le \frac{1}{y-x}\int_x^y f(a)\mathrm{d}a \le \frac{f(x)+f(y)}{2} \tag{2}$$

Lemma 3 (Barbalat Lemma [28]): If $\phi(t) : R \times R$ is a uniformly continuous function for $t \ge 0$ and $\lim_{t\to\infty} \int_0^t \phi(\tau)\mathrm{d}\tau < \infty$, then $\lim_{t\to\infty} \phi(t) = 0$.

Consider the delay differential equation:

$$\dot{x}(t) = f(t, x_t), \quad t \ge t_0 \tag{3}$$

where $x(t) \in R^n$ is a system state vector; x_t is the state trajectory transfer operator on the interval $[-\tau, 0]$ and the expression is $x_t(\theta) = x(t+\theta)$. $f(t, x_t)$ fulfills $f(t, 0) = 0$ and is continuous for x_t.

Lemma 4 (Lyapunov-Krasovskii Theorem [29]): Suppose $R\times C$ is mapped to a bounded sets of R^n by $f : R \times C \to R^n$ in (3), and assume that $\chi(s)$, $\Psi(s)$ and $\ell(s)$ are non-decreasing functions with $\chi(0) = \Psi(0) = 0$ and $\chi(s), \Psi(s) > 0$ for $s > 0$. Suppose there is a differentiable and continuous functional $V : R \times C \to R^n$ that satisfies

$$\chi(\|\phi(0)\|) \le V(t, \phi) \le \Psi(\|\phi\|_c) \tag{4}$$

and $\dot{V}(t, \phi) \le -\ell(\|\phi(0)\|)$, then system (4) is uniformly stable.

Moreover, the solution $x = 0$ is globally uniformly asymptotically stable if $\lim_{s\to\infty} \chi(s) = +\infty$. And it is uniformly asymptotically stable if $s > 0, \ell(s) > 0$.

C. Problem Statement

The longitudinal kinematic model of vehicle in the presence of external disturbances can be described as [19] and [21]:

$$\begin{cases} \dot{p}_i(t) = q_i(t) \\ \dot{q}_i(t) = r_i(t) \\ T_i\dot{r}_i(t) + r_i(t) = u_i(t) + \omega_i(t) \end{cases} \tag{5}$$

where $r_i(t)$, $q_i(t)$ and $p_i(t)$ are respectively the acceleration, velocity and position of vehicle i. T_i is the time constant of the driveline, reflecting the heterogeneity of the CVs in the platoon. $\omega_i(t)$ is external disturbance, and $u_i(t)$ is the control input.

Assumption 1: The disturbances are bounded ([19] and [21]), and there is a positive constant $\bar{\omega}$ that satisfies $|\omega_i(t)| < \bar{\omega}$.

The errors related to position, velocity, and acceleration of vehicles i are defined as:

$$\begin{cases} \tilde{p}_i(t) = p_i(t) - p_0(t) + d_{i0} \\ \tilde{q}_i(t) = q_i(t) - q_0(t) \\ \tilde{r}_i(t) = r_i(t) - r_0(t) \end{cases} \tag{6}$$

where d_{i0} is the desired gap between CVs. Here, the VTH policy used in [6] is adopted to determine d_{i0}:

$$d_{i0}(t) = c_{i0}q_0^2(t) + h_{i0}q_0(t) + s_{i0} \tag{7}$$

where c_{i0} and h_{i0} are positive correlation coefficients, s_{i0} is the standstill distance, and $d_{ij} = d_{i0} - d_{j0}$.

Now, the aim of the CV platoon control is formulated as:

$$\lim_{t\to\infty} \|\tilde{p}_i(t)\| = 0, \quad \lim_{t\to\infty} \|\tilde{q}_i(t)\| = 0, \quad \lim_{t\to\infty} \|\tilde{r}_i(t)\| = 0 \tag{8}$$

Remark 1: According to (7), by selecting appropriate parameters, the VTH can be transformed into CS (when $c_{i0} = 0, h_{i0} = 0$) or CTH (when $c_{i0} = 0$) policy. Therefore, the VTH policy is more representative and flexible.

III. Platoon Controller

A. Platoon Control Algorithm

Firstly, when $\omega_i(t) = 0$, the following VTH policy-based platoon controller is developed:

$$\begin{aligned} &u_i^{nom}(t) \\ &= -\sum_{j=1}^{N} k_{ij}[\alpha(q_i(t) - V_i(\Delta x_{ij}(t))) && \text{(9a)} \\ &\quad + \beta_1(q_i(t) - q_j(t - \tau_{ij}(t))) && \text{(9b)} \\ &\quad + \beta_2(p_i(t) - p_j(t - \tau_{ij}(t)) - \tau_{ij}(t)q_0(t - \tau_{i0}(t)) + d_{ij})] && \text{(9c)} \\ &\quad - k_{i0}[\beta_1(q_i(t) - q_0(t - \tau_{i0}(t))) && \text{(9d)} \\ &\quad + \beta_2(p_i(t) - p_0(t - \tau_{i0}(t)) - \tau_{i0}(t)q_0(t - \tau_{i0}(t)) + d_{i0}) && \text{(9e)} \\ &\quad + \beta_3(r_i(t) - r_0(t - \tau_{i0}(t)))] && \text{(9f)} \end{aligned}$$

Authorized licensed use limited to: Zhejiang Lab. Downloaded on May 06,2022 at 00:50:41 UTC from IEEE Xplore. Restrictions apply.

This article has been accepted for inclusion in a future issue of this journal. Content is final as presented, with the exception of pagination.

where $\alpha, \beta_1, \beta_2, \beta_3$ are control parameters; $\tau_{i0}(t)$ and $\tau_{ij}(t)$ are time delays from the leader and vehicle $j (j \neq i, i, j = 1, \ldots, N)$, in general $\tau_{ij}(t) \neq \tau_{ji}(t)$. d_{ij} is defined as (7), and $V_i(\Delta x_{ij}(t))$ is a function utilized to capture the interactions between CVs, and defined as [11]:

$$V_i(\Delta x_{ij}(t)) = W_1 + W_2 \tanh(C_1 \Delta x_{ij}(t) - C_2) \tag{10}$$

where W_1, W_2, C_1, C_2 are positive parameter values, and $\Delta x_{ij}(t)$ is the average bumper to bumper distance. Suppose the vehicle length is l_c, then it can be described as:

$$\Delta x_{ij}(t) = (p_j(t - \tau_{ij}(t)) - p_i(t) - l_c(i-j))/(i-j) \tag{11}$$

To reject the disturbances, an ISM controller is developed and the ISM surface is designed based on (5) and (9) as:

$$\eta_i(t) = \int_0^t \left(T_i \dot{r}_i(\theta) + r_i(\theta) - u_i^{nom}(\theta)\right) \mathrm{d}\theta \tag{12}$$

Then the ISM controller is developed as

$$u_i^{sli}(t) = -\delta \operatorname{sgn}(\eta_i(t)) \tag{13}$$

Therefore, the controller for CV platoon subjected to external disturbances in (5) is formulated as:

$$u_i(t) = u_i^{nom}(t) + u_i^{sli}(t) \tag{14}$$

Remark 2: Compared with [6], the controller in (14) has three extensions: (i) we employ the third-order heterogeneous vehicle model rather than the second-order model, and the acceleration error is embedded into the controller, which can improve the tracking speed, as concluded in [15]–[17]. (ii) the nonlinear motion coupling interactions between vehicles are considered, thereby improving the ride comfort, which has been proved by [10] and [11]. (iii) the external disturbances are also incorporated, which has more practical significance.

B. Convergence Analysis

The convergence analysis of the platoon is performed in steady state. It implies that the leader travels at a constant velocity, i.e., $\dot{q}_0(t) = 0$ ([4] and [6]). Combining (6) and (9), it follows from (5) that:

$$\begin{aligned}\dot{\tilde{r}}_i(t) = &-T_i^{-1} \sum_{j=1}^{N} k_{ij} [\alpha(\tilde{q}_i(t) + V_i(\Delta x_{ij}^*(t)) - V_i(\Delta x_{ij}(t))) \\ &+ \beta_1(\tilde{q}_i(t) - \tilde{q}_j(t - \tau_{ij})) + \beta_2(\tilde{p}_i(t) - \tilde{p}_j(t - \tau_{ij}))] \\ &- k_{i0}[\beta_1 \tilde{q}_i(t) + \beta_2 \tilde{p}_i(t) + \beta_3 \tilde{r}_i(t)] - T_i^{-1} \tilde{r}_i(t)\end{aligned} \tag{15}$$

where $V_i(\Delta x_{ij}^*) = q_0$, $\Delta x_{ij}^*(t) = (d_{ij} - q_0(t)\tau_{ij} - l_c(i-j))/(i-j)$.

Note that $\Delta x_{ij}^*(t) - \Delta x_{ij}(t) = (\tilde{p}_i(t) - \tilde{p}_j(t - \tau_{ij}))/(i-j)$, using Taylor formula to expand (10), and the first-order Taylor approximation is used to denote $V_i(\Delta x_{ij}(t))$, the following result can be obtained:

$$\begin{aligned}V_i(\Delta x_{ij}(t)) = V_i(\Delta x_{ij}^*(t)) - \frac{V_i'(\Delta x_{ij}^*(t))}{(i-j)} \\ \times (\tilde{p}_i(t) - \tilde{p}_j(t - \tau_{ij}))\end{aligned} \tag{16}$$

Define $\psi_{ij} = V_i'(\Delta x_{ij}^*(t))/(i-j)$, so we can write (15) as:

$$\begin{aligned}\dot{\tilde{r}}_i(t) = &-T_i^{-1} \sum_{j=1}^{N} k_{ij} [(\alpha + \beta_1)\tilde{q}_i(t) - \beta_1 \tilde{q}_j(t - \tau_{ij}) \\ &- (\alpha \psi_{ij} + \beta_2)(\tilde{p}_j(t - \tau_{ij}) - \tilde{p}_i(t))] \\ &- T_i^{-1} k_{i0}[\beta_1 \tilde{q}_i(t) + \beta_2 \tilde{p}_i(t) + \beta_3 \tilde{r}_i(t)] - T_i^{-1} \tilde{r}_i(t)\end{aligned} \tag{17}$$

Let error vectors $\tilde{p} = [\tilde{p}_1, \ldots, \tilde{p}_N]^{\mathrm{T}}$, $\tilde{q} = [\tilde{q}_1, \ldots, \tilde{q}_N]^{\mathrm{T}}$, $\tilde{r} = [\tilde{r}_1, \ldots, \tilde{r}_N]^{\mathrm{T}}$, $\tilde{\kappa} = [\tilde{p}, \tilde{q}, \tilde{r}]^{\mathrm{T}}$ and $\tau_n(t), n = 1, \ldots, m (m \leq N(N-1))$ corresponding to the sequence $\{\tau_{ij}(t) : i, j = 1, \ldots, N, i \neq j\}$, then we have:

$$\dot{\tilde{\kappa}}(t) = C_0 \tilde{\kappa}(t) + \sum_{n=1}^{m} C_n \tilde{\kappa}(t - \tau_n(t)) \tag{18}$$

with

$$\begin{aligned}C_0 &= \begin{bmatrix} 0_N & I_N & 0_N \\ 0_N & 0_N & I_N \\ -TH_p & -TH_v & -TH_a \end{bmatrix}, \\ C_n &= \begin{bmatrix} 0_N & 0_N & 0_N \\ 0_N & 0_N & 0_N \\ TH_{n,p} & TH_{n,v} & 0_N \end{bmatrix}\end{aligned} \tag{19}$$

where I_N and 0_N are identity matrix and zero matrix with dimension N respectively, and:

$$T = \operatorname{diag}\{T_1^{-1}, T_2^{-1}, \ldots, T_N^{-1}\} \tag{20}$$

$$H_p = \operatorname{diag}(h_{p1}, \ldots, h_{pN}),$$

$$h_{pi} = \sum_{j=1}^{N} k_{ij}(\alpha \psi_{ij} + \beta_2) + k_{i0}\beta_2 \tag{21}$$

$$H_v = \operatorname{diag}(h_{v1}, \ldots, h_{vN}),$$

$$h_{vi} = \sum_{j=1}^{N} k_{ij}(\alpha + \beta_1) + k_{i0}\beta_1 \tag{22}$$

$$H_a = \operatorname{diag}(h_{a1}, h_{a2}, \ldots, h_{aN}), h_{ai} = k_{i0}\beta_3 \tag{23}$$

$$H_{n,p} = \operatorname{diag}(h_{ij,p})_{N \times N}, H_{n,v} = \operatorname{diag}(h_{ij,v})_{N \times N} \tag{24}$$

with

$$\begin{aligned}h_{ij,p} &= \begin{cases} 0, & j = i \\ 0, & j \neq i, \tau_{ij}(\cdot) \neq \tau_n(\cdot) \\ k_{ij}(\alpha \psi_{ij} + \beta_2), & \tau_{ij}(\cdot) = \tau_n(\cdot), \end{cases} \\ h_{ij,v} &= \begin{cases} 0, & j = i \\ 0, & j \neq i, \tau_{ij}(\cdot) \neq \tau_n(\cdot) \\ k_{ij}\beta_1, & \tau_{ij}(\cdot) = \tau_n(\cdot) \end{cases}\end{aligned} \tag{25}$$

From Newton-Leibniz formula, we obtain:

$$\tilde{\kappa}(t) = \tilde{\kappa}(t - \tau_n(t)) + \int_{-\tau_n(t)}^{0} \dot{\tilde{\kappa}}(t+s) \mathrm{d}s \tag{26}$$

Substituting (18) into (26), we get:

$$\tilde{\kappa}(t) = \tilde{\kappa}(t - \tau_n(t)) + \sum_{g=0}^{m} C_g \int_{-\tau_n(t)}^{0} \dot{\tilde{\kappa}}(t + s - \tau_g(t+s)) \mathrm{d}s \tag{27}$$

Authorized licensed use limited to: Zhejiang Lab. Downloaded on May 06,2022 at 00:50:41 UTC from IEEE Xplore. Restrictions apply.

This article has been accepted for inclusion in a future issue of this journal. Content is final as presented, with the exception of pagination.

Here we have $\tau_0(t+s) \equiv 0$ and C_g is defined in (19), so we know that $C_n C_g = 0$ when $g \neq 0$, we can write (18) as:

$$\dot{\tilde{\kappa}}(t) = E\tilde{\kappa}(t) - \sum_{n=1}^{m} A_n \int_{-\tau_n(t)}^{0} \tilde{\kappa}(t+s)\mathrm{d}s \tag{28}$$

with

$$E = C_0 + \sum_{n=1}^{m} C_n = \begin{bmatrix} 0_N & I_N & 0_N \\ 0_N & 0_N & I_N \\ -T\hat{H}_p & -T\hat{H}_v & -TH_a \end{bmatrix} \tag{29}$$

$$A_n = C_n C_0 = \begin{bmatrix} 0_N & 0_N & 0_N \\ 0_N & 0_N & 0_N \\ 0_N & TH_{n,p} & TH_{n,v} \end{bmatrix} \tag{30}$$

where $\hat{H}_p = H_p - \sum_{n=1}^{m} H_{n,p}$, $\hat{H}_v = H_v - \sum_{n=1}^{m} H_{n,v}$.

Theorem 1: The matric E in (28) is Hurwitz stable if and only if the parameters satisfy $\alpha > 0, \beta_1 > 0, \beta_2 > 0$, $\beta_3 > 0$ such that D_{1i}, D_{2i} and D_{3i} for E are positive.

Proof: See part A of Appendix.

Theorem 2: Under (9) without disturbances, for (18), if $\alpha, \beta_1, \beta_2, \beta_3$ in (9) satisfy Theorem 1 and suppose the time delay is bounded, i.e., $0 \leq \dot{\tau}_n(t) \leq d_n (d_n \leq 1), 0 \leq \tau_n(t) \leq \tau^*$ [14], then we have:

$$\lim_{t\to\infty} \tilde{\kappa}(t) = 0 \tag{31}$$

Proof: See part B of Appendix.

Remark 3: Note that the typical average end-to-end communication delay in wireless networks is of the order of hundredths of a second and it depends on specific applications and related communication devices [28], [30]. Therefore, it is reasonable that the time delay is assumed to be bounded.

Theorem 3: Under (14), if $\delta > \bar{\omega}$, then the ISM surface can reach $\eta(t) = 0$ in finite time in spite of disturbances.

Proof: See part C of Appendix.

Remark 4: When $\eta(t) = \dot{\eta}(t) = 0$, it is obvious that the controller (14) will turn to (9), as summarized in Theorem 2, (31) still holds in spite of disturbances. Furthermore, $\eta(t) = \dot{\eta}(t) = 0$ implies that $\delta\mathrm{sgn}(\eta(t)) = \omega(t)$. Therefore, ISM controller (13) is similar to a disturbance observer (DO).

C. String Stability Analysis

Definition 1 ([28]): Origin $x_i = 0$, with $i \in N$ and (15), is string stable if given any $\theta > 0$, there exits $\rho > 0$ such that

$$||e_i(0)||_\infty < \theta \Rightarrow \sup_i ||e_i(\cdot)||_\infty < \rho \tag{32}$$

Theorem4: Under the PLF topology, the string stability of the CV platoon is ensured under the developed controller (14).

Proof: See part D of Appendix.

IV. Numerical Simulation

This section provides simulations to test the performance of the proposed controller under the PLF topology. According to Fig. 1, the heterogeneous platoon is composed of seven CVs, including one leader and six followers.

TABLE I
PARAMETERS FOR THE SIMULATION

Parameter	Value	Parameter	Value
C_1	0.13m^{-1}	β_2	1s^{-1}
C_2	1.59	β_3	5
W_1	6.75m/s	$c_{i,i-1}$	0.0448s^2/m
W_2	7.91m/s	$h_{i,i-1}$	0.0019s
α	0.1s^{-1}	$s_{i,i-1}$	8m
β_1	6s^{-2}	δ	3

A. Simulation Setting

In simulation, the time step is 0.01s. The external disturbances $\omega_i(t) = 2.5\sin(0.1it + \pi/i)$, the initial positions $p(0) = [0, 14, 28.5, 43.5, 59, 75, 91.5]^{\mathrm{T}}$m. The initial velocity and acceleration of followers are set to 10m/s and 0m/s^2 respectively. The velocity of the leader is set as (33).

$$q_0(t) = \begin{cases} 10\text{m/s} & 0 \leq t \leq 15\text{s} \\ (10 + \dfrac{12}{1+e^{-0.45t+20}})\text{m/s} & 15\text{s} \leq t \leq 70\text{s} \\ 22\text{m/s} & 70\text{s} \leq t \leq 75\text{s} \\ (22 - \dfrac{12}{1+e^{-0.4t+42}})\text{m/s} & \text{otherwise} \end{cases} \tag{33}$$

Suppose the length of CVs is 4m. The time constants of the driveline are set to $T_i = [0.5, 0.4, 0.3, 0.4, 0.35, 0.5]^{\mathrm{T}}$s (see [15]). The upper bound $\tau^*$is 0.2s according to (49) and all delays are set to the maximum value. The values of parameters in (7) and (10) can refer to [6] and [11]. The control gains are selected based on Theorems 1 and 3. Table I lists the specific values.

B. Platoon Formation and Maintenance

Two cases are considered: no disturbances and time-varying disturbances, and the results are presented in Figs. 2-7. The results suggest that velocities of the followers can reach the same velocity as the leader, and the platoon moves at the same velocity eventually (see Figs. 2(a), 4(a) and 6(a)). And the accelerations of the followers eventually reach to the desired zero (see Figs. 5(a) and 7(a)). Moreover, the position error in Fig. 2(c) illustrate that all followers can maintain the desired distance and track the leader stably.

In conclusion, Figs. 2-7 show that the proposed controller can effectively eliminate the impact of external disturbances on the CV platoon, and eventually form a stable platoon.

C. Comparison to Existing Methods

Next, we compare the proposed third-order VTH-based controller with second-order VTH-based controller in [6] and third-order CTH-based controller in [18].

The results without disturbances are shown in Figs. 3-5. The distance profiles $(p_{i-1}(t) - p_i(t))$ in Fig. 3 show that VTH spacing policy can adjust the desired inter-vehicle spacing more flexibly and reasonably according to the vehicle velocity. Specifically, compared with the CTH-based controller in [18], the VTH-based controllers in this article and [6] can promote

Authorized licensed use limited to: Zhejiang Lab. Downloaded on May 06,2022 at 00:50:41 UTC from IEEE Xplore. Restrictions apply.

This article has been accepted for inclusion in a future issue of this journal. Content is final as presented, with the exception of pagination.

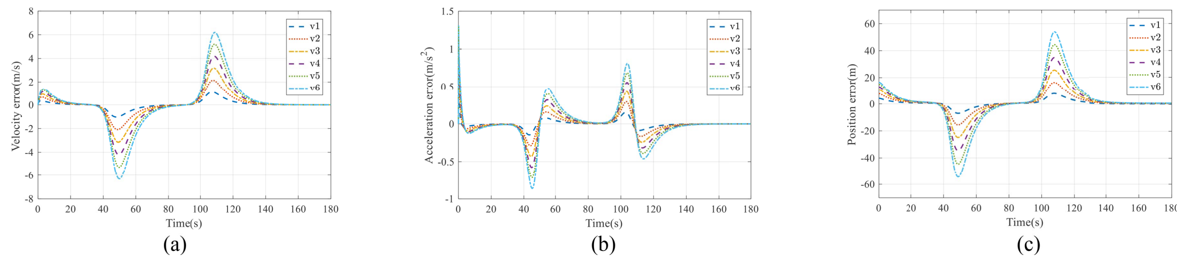

Fig. 2. Driving cycle with the proposed controller: (a) velocity error, (b) acceleration error, (c) position error.

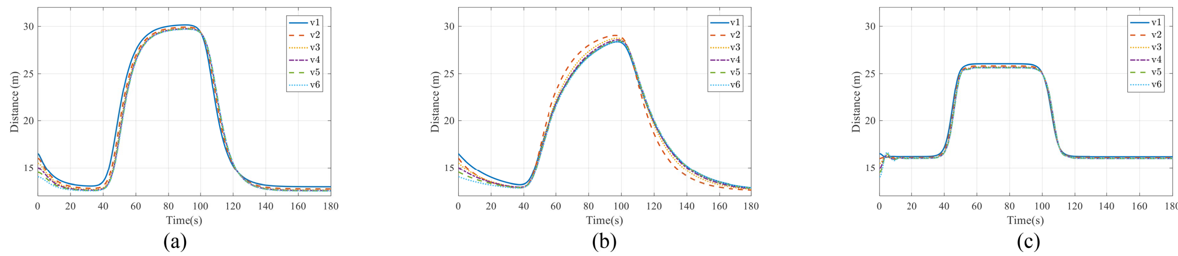

Fig. 3. Distance without disturbances: (a) the proposed controller, (b) controller in [6], (c) controller in [18].

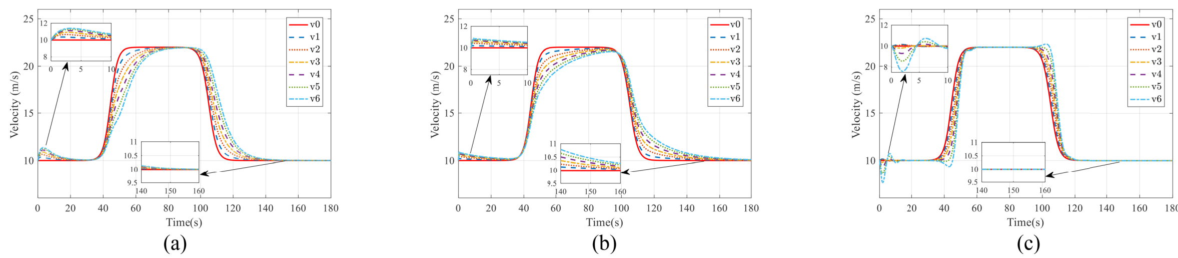

Fig. 4. Velocity without disturbances: (a) the proposed controller, (b) controller in [6], (c) controller in [18].

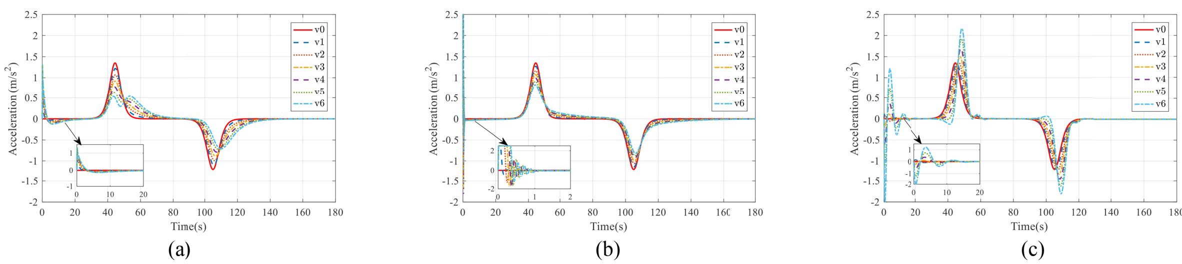

Fig. 5. Acceleration without disturbances: (a) the proposed controller, (b) controller in [6], (c) controller in [18].

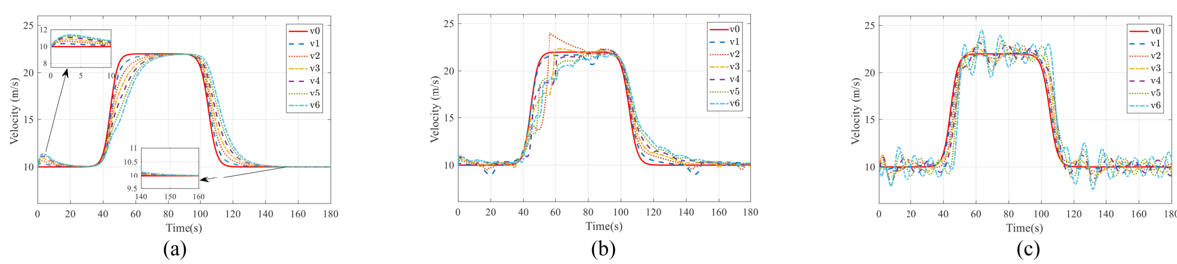

Fig. 6. Velocity with time-varying disturbances: (a) the proposed controller, (b) controller in [6], (c) controller in [18].

a larger safety spacing between CVs at high velocity (when 50s $\le t \le$ 120s) to avoid collision, and also maintain a smaller spacing between CVs at low velocity (when 0s $\le t \le$ 50s and 120s $\le t \le$ 180s) to increase road capacity. It implies that when a vehicle is traveling at high velocity and an emergency occurs, then the braking distance of the vehicle to stop needs large enough to avoid rear-end collision. Therefore, under the proposed VTH-based controller, the risk of rear-end collision will reduce due to the larger inter-vehicle spacing. On the other hand, when a vehicle is traveling at low velocity, then the road capacity will improve due to the smaller inter-vehicle spacing. This illustrates that the VTH policy is more flexible and effective than the CTH policy. Comparing the velocity of Figs. 4(a), 4(b) and 4(c), it indicates that the convergence speed under the controllers (14) and [18] is faster than that under the controller in [6]. This is

Authorized licensed use limited to: Zhejiang Lab. Downloaded on May 06,2022 at 00:50:41 UTC from IEEE Xplore. Restrictions apply.

This article has been accepted for inclusion in a future issue of this journal. Content is final as presented, with the exception of pagination.

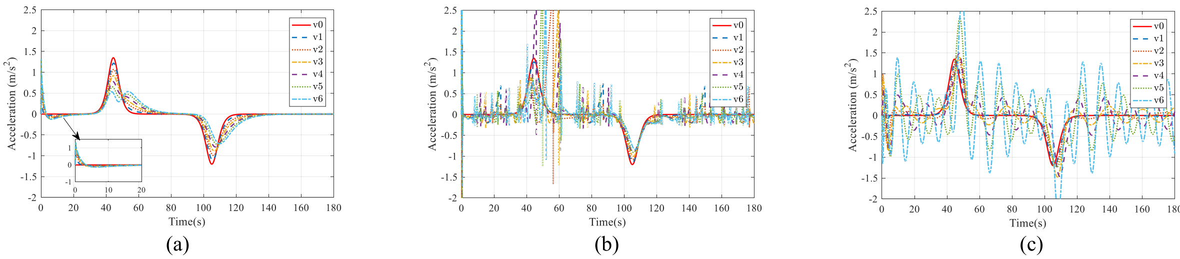

Fig. 7. Acceleration with time-varying disturbances: (a) the proposed controller, (b) controller in [6], (c) controller in [18].

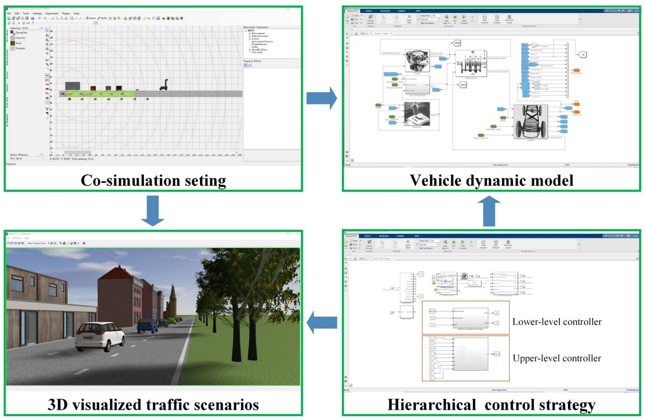

Fig. 8. Framework of co-simulation.

because the acceleration differences are incorporated into the controller design and thus effectively improving the tracking speed of the platoon, which is consistent with the conclusion in [17]. Moreover, the maximum amplitude of acceleration in Figs. 5(b) and 5(c) are 2.5m/s^2 and 2.1m/s^2, respectively. And at the beginning, it is evident that fluctuations exist with the acceleration in Figs. 5(b) and 5(c). However, under the proposed controller (14), the acceleration in Fig. 5(a) is smooth and the maximum amplitude is 1.3m/s^2. This is because the nonlinear motion coupling interactions (9a) between CVs are incorporated, which could avoid unreasonable acceleration rate and improve the ride comfort.

The results with time-varying external disturbances are shown in Figs. 6 and 7. It is obvious that under the proposed controller (14), the disturbances are effectively suppressed and the platoon finally reaches a consensus and stable state (see Figs. 6(a) and 7(a)). On the contrast, under the controllers developed in [6] and [18], the platoon is always in an unstable state in terms of Figs. 6(b), 6(c), 7(b) and 7(c), and even leading to collision and separation. Therefore, the disturbances rejection and the smoothness of the proposed controller are better than those in [6] and [18].

V. Co-Simulation

This section conducts the co-simulation in MATLAB/Simulink and PreScan to verify the effectiveness of the proposed controller in a more realistic scenario. Fig. 8 presents the framework of the co-simulation. In particular, MATLAB/Simulink is used to build the control algorithm. PreScan is used to model the traffic scenario

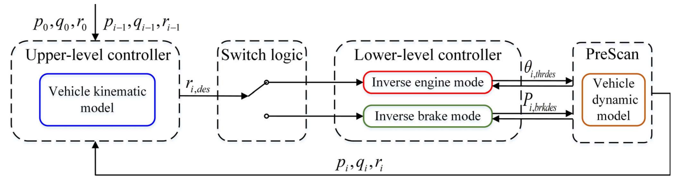

Fig. 9. Hierarchical control of vehicle platoon.

and provides the vehicle model, on-board sensors and 3D visualized display.

To perform the co-simulation, a hierarchical platoon control strategy is adopted, as depicted in Fig. 9. The upper-level controller determines the desired acceleration $r_{i,des}$ according to the kinematic model (5) and controller (14), then the lower-level controller generates the desired throttle opening $\theta_{i,thrdes}$ or brake pressure $P_{i,brkdes}$ by using the following inverse model [13]:

$$\begin{aligned} T_{i,des}(t) &= R_i(m_i r_{i,des} + C_{A,i} q_i^2(t) + m_i g f)/\varpi_{T,i} \\ \theta_{i,thrdes}(t) &= MAP^{-1}(w_e, T_{i,des}) \\ P_{i,brkdes}(t) &= R_i(m_i r_{i,des} + C_{A,i} q_i^2(t) + m_i g f)/K_b \end{aligned} \quad (34)$$

In the co-simulation, all parameters and condition settings are the same as in Section IV. The parameters in (34) are set as: $m_i = 1532$kg, $\varpi_{T,i} = 0.9$, $C_{A,i} = 0.492$kg/m, $g = 9.8$m/s^2, $f = 0.01$, $R_i = 0.3$m, and $K_b = 426$N·m/MPa. The results are shown in Fig. 10. The velocity in Fig. 10(a) shows that the following vehicles can track the leading vehicle smoothly, and finally maintain at a constant velocity of 10m/s. Fig. 10(b) shows that the acceleration of all followers can reach zero eventually, and the maximum acceleration/deceleration amplitude is 1.3m/s^2, which is the same as in Section IV. Besides, Fig. 10(c) indicates that position errors of the followers finally converge to zero, that is, all vehicles finally keep the desired spacing. And the throttle angle and brake pressure are respectively shown in Figs. 10(d) and 10(e).

VI. Experiment

This section provides experiments with the IMVs to test the practical feasibility of the developed controller.

A. Experimental Setup

Fig. 11 shows the test platform including three IMVs, a cloud server, a laptop computer, and a straight road with length of 16m and width of 0.35m. The IMV is mainly composed of seven modules, and their corresponding functions are shown in Table II. The motion data of IMVs received by

Authorized licensed use limited to: Zhejiang Lab. Downloaded on May 06,2022 at 00:50:41 UTC from IEEE Xplore. Restrictions apply.

This article has been accepted for inclusion in a future issue of this journal. Content is final as presented, with the exception of pagination.

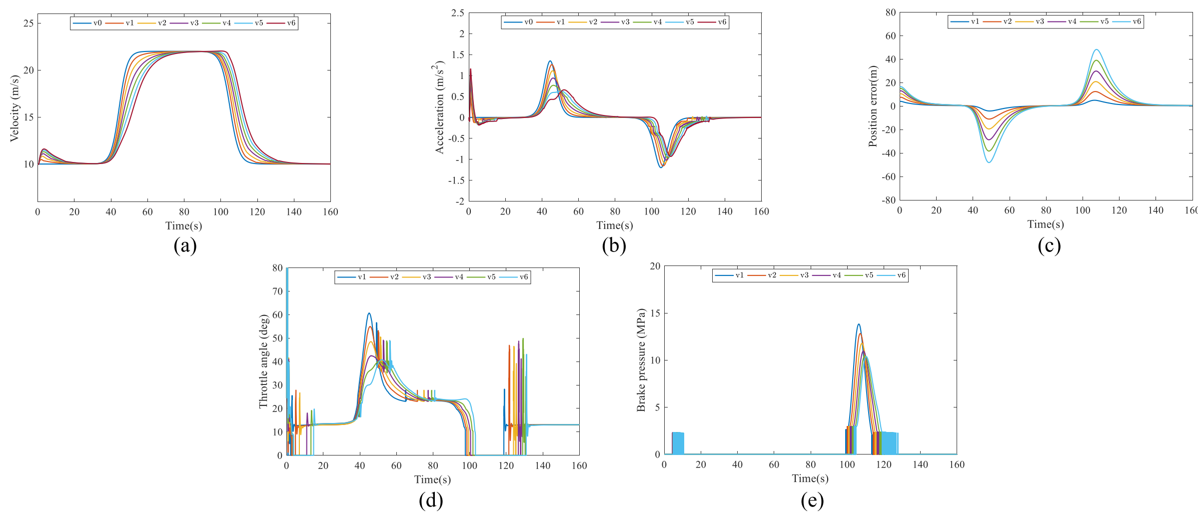

Fig. 10. Co-simulation results: (a) velocity, (b) acceleration, (c) position error, (d) throttle angle, (e) brake pressure.

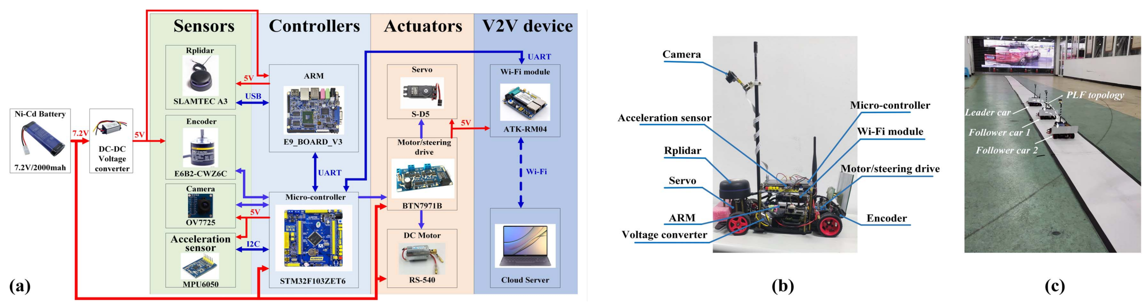

Fig. 11. The test platform of IMV: (a) functional diagram of IMV, (b) physical drawing of IMV, (c) experimental scene.

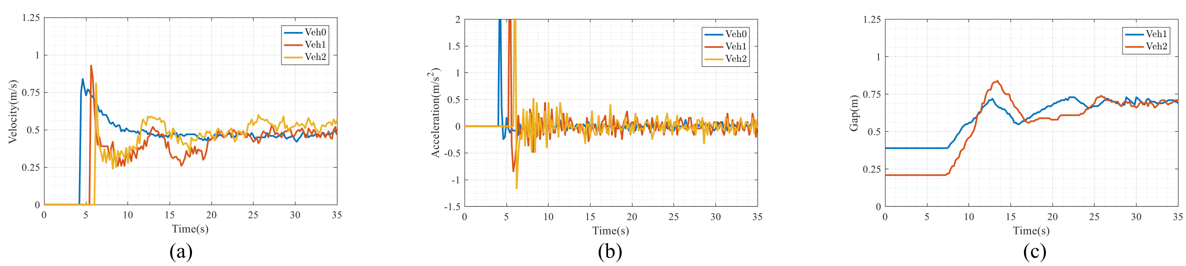

Fig. 12. Experimental results: (a) velocity, (b) acceleration, (c) gap.

TABLE II
THE FUNCTION OF EACH IMV MODULE

Module	Function
Camera module	Sense and collect road information
Wi-Fi module	Communication between IMVs, and between IMVs and cloud server.
Rplidar module	Detect the distance between IMVs.
Encoder module	Measure the velocity of IMVs.
Tri-axis acceleration sensor module	Measure the acceleration of IMVs.
E9 card computer module	Drive the Rplidar and process distance data.
Micro-controller module	Load the control algorithm.

the cloud server through the Wi-Fi module will be stored in the MySQL database for the following experimental analysis.

B. Experimental Results

To perform the experiments, the proposed controller in (14) is loaded into the Micro-controller of IMV using the C language. Then, the Micro-controller calculates the control commands according to the received data to drive the motor and servo. The parameters $\alpha_i = 0.01$, $\beta_{i1} = 4.5$, $\beta_{i2} = 1.2$, $\beta_{i3} = 3.5$, $\delta = 4$ and $s_{i,i-1} = 0.7\text{m}(i = 1, 2)$, other parameters are the same as those in Table I. According to (7), the desired spacing between two adjacent IMVs is 0.71m. And the desired velocity of the leader is set as 0.5m/s. The initial spacing between IMVs is set as 0.2m and 0.4m, respectively. In the experiment, all IMVs start from a zero initial state.

Fig. 12 presents the experimental results. Figs. 12(a) and 12(c) show that the velocities of following IMVs are almost at about 0.5m/s, and the inter-vehicle gaps between IMVs converge to 0.69m, respectively. Fig. 12(b) shows that the amplitude of acceleration is acceptable. The experimental results shown in Fig. 12 allow the verification of the effectiveness of the proposed controller.

Authorized licensed use limited to: Zhejiang Lab. Downloaded on May 06,2022 at 00:50:41 UTC from IEEE Xplore. Restrictions apply.

This article has been accepted for inclusion in a future issue of this journal. Content is final as presented, with the exception of pagination.

VII. Conclusion

In this article, a novel third-order VTH policy based platoon controller is designed by considering the nonlinear motion coupling interactions and time delays as well as external disturbances. Then, the asymptotic stability and string stability for the CV platoon are proved respectively by rigorous theoretical analysis. Further, extensive simulations and co-simulations in MATLAB/Simulink and PreScan are performed to validate the designed controller. More importantly, experiments with IMVs are further conducted to verify the feasibility of the developed controller.

The limitations of this study are as follows: the model used for vehicle is kinematic model, rather than dynamic model, which cannot fully characterize the vehicle. Moreover, the IMVs used in the experiment cannot reflect the physical characteristics of real vehicles roundly. Future efforts can be made in these aspects.

Appendix

A. Proof of Theorem 1

Assuming that λ is any eigenvalue of matrix E, then the characteristic polynomial of E is:

$$\det(\lambda I_{3N} - E) = \prod_{i=1}^{N} (\lambda^3 + T_i^{-1}(k_{i0}\beta_3 + 1)\lambda^2 + T_i^{-1}a_i\lambda + T_i^{-1}b_i) \tag{35}$$

Then the "north-westerly" minors of the Bilharz matrix [15] related to (35) are:

$$\begin{aligned}
D_{1i} &= T_i^{-1}(k_{i0}\beta_3 + 1)\\
D_{2i} &= T_i^{-2}(k_{i0}\beta_3 + 1)(T_i^{-1}(k_{i0}\beta_3 + 1)\mathrm{Re}(a_i) - \mathrm{Re}(b_i))\\
&\quad - T_i^{-2}(\mathrm{Im}(a_i))^2\\
D_{3i} &= -T_i^{-4}(\mathrm{Im}(a_i)^3\mathrm{Im}(b_i) + \mathrm{Re}(b_i)(\mathrm{Im}(a_i))^2\mathrm{Re}(a_i))\\
&\quad + T_i^{-3}(\mathrm{Re}(b_i))^2\\
&\quad - T_i^{-4}(k_{i0}\beta_3 + 1)(2(\mathrm{Re}(b_i))^2\mathrm{Re}(a_i)\\
&\quad + \mathrm{Im}(b_i)\mathrm{Re}(b_i)\mathrm{Im}(a_i))\\
&\quad + T_i^{5}(k_{i0}\beta_3 + 1)^2((\mathrm{Re}(a_i))^2\mathrm{Re}(b_i)\\
&\quad + \mathrm{Im}(a_i)\mathrm{Re}(a_i)\mathrm{Re}(b_i)\\
&\quad + (k_{i0}\beta_3 + 1)(\mathrm{Im}(b_i))^2)
\end{aligned} \tag{36}$$

where a_i and b_i are respectively the i-th eigenvalues of $\hat{H}_p$ and $\hat{H}_v$. According to Lemma 1, when D_{1i}, D_{2i}, D_{3i} are positive, it can be concluded that E is Hurwitz stable under the conditions: $\alpha > 0, \beta_1 > 0, \beta_2 > 0, \beta_3 > 0$.

B. Proof of Theorem 2

(Sufficiency): choose the Lyapunov-Krasovskii function:

$$V_1(\tilde{\kappa}(t)) = \tilde{\kappa}^{\mathrm{T}}(t)Q\tilde{\kappa}(t) + \sum_{n=1}^{m}\int_{t-\tau_n(t)}^{t}\tilde{\kappa}^{\mathrm{T}}(s)B_n\tilde{\kappa}(s)\mathrm{d}s \tag{37}$$

with $Q = Q^{\mathrm{T}} > 0$ and $B_n > 0$. Define

$$h(\tilde{\kappa}(t)) = \tilde{\kappa}^{\mathrm{T}}(t)Q\tilde{\kappa}(t) \tag{38}$$

$$g(\tilde{\kappa}(t-\tau^*)) = \tilde{\kappa}^{\mathrm{T}}Q\tilde{\kappa} + \sum_{n=1}^{m}\int_{t-\tau^*}^{t}\tilde{\kappa}^{\mathrm{T}}(s)B_n\tilde{\kappa}(s)\mathrm{d}s \tag{39}$$

Then the following condition is satisfied:

$$h(\tilde{\kappa}(t)) \le V_1(\tilde{\kappa}(t)) \le g(\tilde{\kappa}(t-\tau^*)) \tag{40}$$

By differentiating (37) and combining (28) yields:

$$\begin{aligned}
\dot{V}_1(\tilde{\kappa}) &= \tilde{\kappa}^{\mathrm{T}}(E^{\mathrm{T}}Q + QE + \sum_{n=1}^{m}B_n)\tilde{\kappa}\\
&\quad - 2\tilde{\kappa}^{\mathrm{T}}Q\sum_{n=1}^{m}\int_{-\tau_n(t)}^{0}A_n\tilde{\kappa}(t+s)\mathrm{d}s\\
&\quad - \sum_{n=1}^{m}(1-\dot{\tau}_n)\tilde{\kappa}^{\mathrm{T}}(t-\tau_n(t))B_n\tilde{\kappa}(t-\tau_n(t))
\end{aligned} \tag{41}$$

For any positive definite matrix and any vector, it holds that $2a^{\mathrm{T}}d \le d^{\mathrm{T}}H^{-1}d + a^{\mathrm{T}}Ha$, then we have

$$\begin{aligned}
&2\tilde{\kappa}^{\mathrm{T}}(t)Q\sum_{n=1}^{m}\int_{-\tau_n(t)}^{0}A_n\tilde{\kappa}(t+s)\mathrm{d}s\\
&\le \sum_{n=1}^{m}\int_{-\tau_n(t)}^{0}\Big(\tilde{\kappa}^{\mathrm{T}}(t+s)Q\tilde{\kappa}(t+s)\\
&\quad + \tilde{\kappa}^{\mathrm{T}}(t)QA_nQ^{-1}A_n^{\mathrm{T}}Q^{\mathrm{T}}\tilde{\kappa}(t)\Big)\mathrm{d}s
\end{aligned} \tag{42}$$

Based on Theorem 1, when matric E is Hurwitz stable, there exists positive definite matrix Q and M that satisfy

$$E^{\mathrm{T}}Q + QE = -M \tag{43}$$

Employing Lemma 2, we have

$$\begin{aligned}
&\int_{-\tau_n(t)}^{0}\tilde{\kappa}^{\mathrm{T}}(t+s)Q\tilde{\kappa}(t+s)\mathrm{d}s\\
&\quad \le 0.5\tau^*(\tilde{\kappa}^{\mathrm{T}}(t)Q\tilde{\kappa}(t) + \tilde{\kappa}^{\mathrm{T}}(t-\tau_n(t))Q\tilde{\kappa}(t-\tau_n(t)))
\end{aligned} \tag{44}$$

Then based on the above, (41) can ultimately be reduced to

$$\begin{aligned}
\dot{V}_1(\tilde{\kappa}) &\le -\tilde{\kappa}^{\mathrm{T}}M\tilde{\kappa} + \tilde{\kappa}^{\mathrm{T}}\sum_{n=1}^{m}B_n\tilde{\kappa} - \sum_{n=1}^{m}[\tau^*\tilde{\kappa}^{\mathrm{T}}QA_nQ^{-1}A_n^{\mathrm{T}}Q^{\mathrm{T}}\tilde{\kappa}\\
&\quad + 0.5\tau^*(\tilde{\kappa}^{\mathrm{T}}Q\tilde{\kappa} + \tilde{\kappa}^{\mathrm{T}}(t-\tau_n(t))Q\tilde{\kappa}(t-\tau_n(t)))]\\
&\quad - \sum_{n=1}^{m}(1-\dot{\tau}_n)\tilde{\kappa}^{\mathrm{T}}(t-\tau_n(t))B_n\tilde{\kappa}(t-\tau_n(t))
\end{aligned} \tag{45}$$

Let $\xi(t) = [\tilde{\kappa}(t), \tilde{\kappa}(t-\tau_1(t)), \ldots, \tilde{\kappa}(t-\tau_m(t))]^{\mathrm{T}}$, we have:

$$\dot{V}_1(\tilde{\kappa}) \le \xi^{\mathrm{T}}(t)\Omega\xi(t) \tag{46}$$

with

$$\Omega = \mathrm{diag}(\Omega_0, \Omega_1, \cdots, \Omega_m) \tag{47}$$

Authorized licensed use limited to: Zhejiang Lab. Downloaded on May 06,2022 at 00:50:41 UTC from IEEE Xplore. Restrictions apply.

This article has been accepted for inclusion in a future issue of this journal. Content is final as presented, with the exception of pagination.

where

$$\begin{aligned}\Omega_0 &= -M + \sum_{n=1}^{m}\Big(B_n - \tau^* Q A_n Q^{-1} A_n^{\mathrm{T}} Q^{\mathrm{T}} - 0.5\tau^* Q\Big)\\ \Omega_1 &= -0.5\tau^* Q - B_1(1-d_1)\\ &\vdots\\ \Omega_m &= -0.5\tau^* Q - B_m(1-d_m)\end{aligned} \tag{48}$$

According to Lyapunov-Krasovskii theorem, to ensure that system (18) is stable, then matrix Ω must be negative definite. It is easy to induce that $\Omega_i = (1, \ldots, m)$ defined in (48) are negative definitive. So as long as Ω_0 is negative definitive, then Ω is negative definitive. Consequently, we can derive:

$$\tau^* < ||\sum_{n=1}^{m} B_n - M|| \Big/ ||\sum_{n=1}^{m} Q A_n Q^{-1} A_n^{\mathrm{T}} Q^{\mathrm{T}} + 0.5Q|| \tag{49}$$

(Necessity): For any delay $0 \leq \tau_n(t) \leq \tau^*$, suppose $\tau_n(t) = 0$, then $\dot{\tilde{\kappa}}(t) = E\tilde{\kappa}(t)$ is asymptotically stable when E is Hurwitz. Hence, Theorem 2 is proved.

C. Proof of Theorem 3

First define some state vectors as follows:

$$p(t) = [p_1(t), \cdots, p_N(t)]^{\mathrm{T}}, q(t) = [q_1(t), \cdots, q_N(t)]^{\mathrm{T}} \tag{50}$$

$$\eta(t) = [\eta_1(t), \cdots, \eta_N(t)]^{\mathrm{T}}, u(t) = [u_1(t), \cdots, u_N(t)]^{\mathrm{T}} \tag{51}$$

$$\begin{aligned}u^{nom}(t) &= [u_1^{nom}(t), \cdots, u_N^{nom}(t)]^{\mathrm{T}},\\ \omega(t) &= [\omega_1(t), \cdots, \omega_N(t)]^{\mathrm{T}}\end{aligned} \tag{52}$$

Then (12) and (14) can be rewritten as:

$$\eta(t) = \int_0^t \Big(T^{-1}\dot{q}(\theta) + q(\theta) - u^{nom}(\theta)\Big)\mathrm{d}\theta \tag{53}$$

$$u(t) = u^{nom}(t) - \delta\,\mathrm{sgn}(\eta) \tag{54}$$

Define $V_2(t) = \frac{1}{2}\eta^{\mathrm{T}}(t)\eta(t)$, and we have:

$$\begin{aligned}\dot{V}_2(t) &= -\delta\,\|\eta\|_1 + \eta^{\mathrm{T}}\omega \leq -\delta\,\|\eta\|_1 + \bar{\omega}\,\|\eta\|_1\\ &\leq -(\delta - \bar{\omega})\sqrt{2V_2}\end{aligned} \tag{55}$$

If $\delta > \bar{\omega}$, we have $\dot{V}_2(t) < 0$. Hence, the ISM can reach $\eta(t) = 0$ in finite time. The proof is complete.

D. Proof of Theorem 4

The spacing error is defined as:

$$e_i(t) = p_{i-1}(t) - p_i(t) + d_{i,i-1} \tag{56}$$

Then we obtain $\ddot{e}_i(t) = r_{i-1}(t) - r_i(t)$, given the fact that the accelerations of $r_i(t)$ and $r_{i-1}(t)$ are bounded, it indicates that $\ddot{e}_i(t) \in \mathcal{L}_\infty$, so $\dot{e}_i(t)$ is uniformly continuous. Besides,

$$\int_0^\infty |\dot{e}_i(t)|\mathrm{d}t = |e_i(\infty)| - |e_i(0)| < \infty \tag{57}$$

Therefore, $\dot{e}_i(t) \in \mathcal{L}_2$. We further have $\lim_{t\to\infty} \dot{e}_i(t) = 0$ according to Lemma 3. Consequently, we get $\dot{e}_i(t) \in \mathcal{L}_\infty$. Similarly, we have $e_i(t) \in \mathcal{L}_2$. And we further have $\lim_{t\to\infty} e_i(t) = 0$ based on Lemma 3.

If $\xi > 0$, then $||e_i(0)||_\infty = \sup_i |e_i(0)| = 0 < \xi$. Moreover, consider that $\lim_{t\to\infty} e_i(t) = 0, e_i(0) = 0, e_i(t) \in \mathcal{L}_2$. Hence,$\exists \nu, \gamma > 0,\ s.t.\ \sup_{i, t\in[0,\infty)} |e_i(t)| = \nu < \gamma$. Therefore, the string stability is proved according to Definition 1.

References

[1] Y. Chen, J. Zha, and J. Wang, "An autonomous T-intersection driving strategy considering oncoming vehicles based on connected vehicle technology," *IEEE/ASME Trans. Mechatronics.*, vol. 24, no. 6, pp. 2779–2790, Dec. 2019.

[2] W. B. Qin and G. Orosz, "Experimental validation on connected cruise control with flexible connectivity topologies," *IEEE/ASME Trans. Mechatronics.*, vol. 24, no. 6, pp. 2791–2802, Dec. 2019.

[3] Y. Li, C. Tang, S. Peeta, and Y. Wang, "Integral-sliding-mode braking control for a connected vehicle platoon: Theory and application," *IEEE Trans. Ind. Electron.*, vol. 66, no. 6, pp. 4618–4628, Jun. 2019.

[4] M. di Bernardo, A. Salvi, and S. Santini, "Distributed consensus strategy for platooning of vehicles in the presence of time-varying heterogeneous communication delays," *IEEE Trans. Intell. Transp. Syst.*, vol. 16, no. 1, pp. 102–112, Feb. 2015.

[5] Y. Li, C. Tang, K. Li, X. He, S. Peeta, and Y. Wang, "Consensus-based cooperative control for multi-platoon under the connected vehicles environment," *IEEE Trans. Intell. Transp. Syst.*, vol. 20, no. 6, pp. 2220–2229, Jun. 2019.

[6] J. Chen, H. Liang, J. Li, and Z. Lv, "Connected automated vehicle platoon control with input saturation and variable time headway strategy," *IEEE Trans. Intell. Transp. Syst.*, vol. 22, no. 8, pp. 4929–4940, Aug. 2021.

[7] D. Jia and D. Ngoduy, "Platoon based cooperative driving model with consideration of realistic inter-vehicle communication," *Transp. Res. C*, vol. 68, pp. 245–264, Sep. 2016.

[8] S. Santini, A. Salvi, A. S. Valente, A. Pescape, M. Segata, and R. L. Cigno, "Platooning maneuvers in vehicular networks: A distributed and consensus-based approach," *IEEE Trans. Intell. Vehicles*, vol. 4, no. 1, pp. 59–72, Mar. 2019.

[9] J. Wang, X. Luo, W. Wong, and X. Guan, "Specified-time vehicular platoon control with flexible safe distance constraint," *IEEE Trans. Veh. Technol*, vol. 68, no. 11, pp. 10489–10503, Nov. 2019.

[10] Y. Li, C. Tang, K. Li, S. Peeta, X. He, and Y. Wang, "Nonlinear finite-time consensus based connected vehicle platoon control under fixed and switching communication topologies," *Transp. Res. C, Emerg. Technol.*, vol. 93, pp. 525–543, Aug. 2018.

[11] Y. Li, C. Tang, S. Peeta, and Y. Wang, "Nonlinear consensus-based connected vehicle platoon control incorporating car-following interactions and heterogeneous time delays," *IEEE Trans. Intell. Transp. Syst.*, vol. 20, no. 6, pp. 2209–2219, Jun. 2019.

[12] J. C. Zegers, E. Semsar-Kazerooni, J. Ploeg, N. Van De Wouw, and H. Nijmeijer, "Consensus control for vehicular platooning with velocity constraints," *IEEE Trans. Control Syst. Technol.*, vol. 26, no. 5, pp. 1592–1605, Jul. 2018.

[13] S. E. Li, X. Qin, K. Li, J. Wang, and B. Xie, "Robustness analysis and controller synthesis of homogeneous vehicular platoons with bounded parameter uncertainty," *IEEE/ASME Trans. Mechatronics*, vol. 22, no. 2, pp. 1014–1025, Apr. 2017.

[14] G. Fiengo, D. G. Lui, A. Petrillo, S. Santini, and M. Tufo, "Distributed robust PID control for leader tracking in uncertain connected ground vehicles with V2V communication delay," *IEEE/ASME Trans. Mechatronics*, vol. 24, no. 3, pp. 1153–1165, Jun. 2019.

[15] S. Alessandro, S. Stefania, and S. V. Antonio, "Design, analysis and performance evaluation of a third order distributed protocol for platooning in the presence of time-varying delays and switching topologies," *Transp. Res. C, Emerg. Technol.*, vol. 80, pp. 360–383, Jul. 2017.

[16] F. Ma *et al.*, "Distributed control of cooperative vehicular platoon with nonideal communication condition," *IEEE Trans. Veh. Technol.*, vol. 69, no. 8, pp. 8207–8220, Aug. 2020.

[17] A. Elahi, A. Alfi, and H. Modares, "H_∞ consensus of homogeneous vehicular platooning systems with packet dropout and communication delay," *IEEE Trans. Syst., Man, Cybern., Syst.*, early access, Apr. 19, 2021, doi: 10.1109/TSMC.2021.3071994.

Authorized licensed use limited to: Zhejiang Lab. Downloaded on May 06,2022 at 00:50:41 UTC from IEEE Xplore. Restrictions apply.

This article has been accepted for inclusion in a future issue of this journal. Content is final as presented, with the exception of pagination.

[18] R. Oliveira, C. Montez, A. Boukerche, and M. S. Wangham, "Co-design of consensus-based approach and reliable communication protocol for vehicular platoon control," *IEEE Trans. Veh. Technol.*, vol. 70, no. 9, pp. 9510–9524, Sep. 2021.

[19] Y. Zhao, Z. Liu, and W. S. Wong, "Resilient platoon control of vehicular cyber physical systems under DoS attacks and multiple disturbances," *IEEE Trans. Intell. Transp. Syst.*, early access, Jul. 28, 2021, doi: 10.1109/TITS.2021.3097356.

[20] Q. Wu, H. Ge, P. Fan, J. Wang, Q. Fan, and Z. Li, "Time-dependent performance analysis of the 802.11p-based platooning communications under disturbance," *IEEE Trans. Veh. Technol.*, vol. 69, no. 12, pp. 15760–15773, Dec. 2020.

[21] X. Ge, S. Xiao, Q. Han, X. Zhang, and D. Ding, "Dynamic event-triggered scheduling and platooning control co-design for automated vehicles over vehicular ad-hoc networks," *IEEE/CAA Journal of Automatica Sinica*, vol. 9, no. 1, pp. 31–46, Jul. 2021, doi: 10.1109/JAS.2021.1004060.

[22] B. Besselink and K. H. Johansson, "String stability and a delay-based spacing policy for vehicle platoons subject to disturbances," *IEEE Trans. Autom. Control*, vol. 62, no. 9, pp. 4376–4391, Sep. 2017.

[23] J. Chen, Y. Zhou, and H. Liang, "Effects of ACC and CACC vehicles on traffic flow based on an improved variable time headway spacing strategy," *IET Intell. Transp. Syst.*, vol. 13, no. 9, pp. 1365–1373, Sep. 2019.

[24] K. Santhanakrishnan and R. Rajamani, "On spacing policies for highway vehicle automation," *IEEE Trans. Intell. Transp. Syst.*, vol. 4, no. 4, pp. 198–204, Dec. 2003.

[25] D. Yanakiev and I. Kanellakopoulos, "Nonlinear spacing policies for automated heavy-duty vehicles," *IEEE Trans. Veh. Technol.*, vol. 47, no. 4, pp. 1365–1377, Nov. 1998.

[26] P. Parks and V. Hahn, *Stability Theory*. Upper Saddle River, NJ, USA: Prentice-Hall, 1992.

[27] J. K. Hale and S. M. V. Lunel, *Introduction to Functional Differential Equations*. New York, NY, USA: Springer-Verlag, 1993.

[28] Y. Li, W. Chen, S. Peeta, and Y. Wang, "Platoon control of connected multi-vehicle systems under V2X communications: Design and experiments," *IEEE Trans. Intell. Transp. Syst.*, vol. 21, no. 5, pp. 1891–1902, May 2020.

[29] K. Gu, V. L. Kharitonov, and J. Chen, *Stability of Time-Delay Systems*. Boston, MA, USA: Birkhäuser, 2003.

[30] B. Caiazzo, D. G. Lui, A. Petrillo, and S. Santini, "Distributed double-layer control for coordination of multi-platoons approaching road restriction in the presence of IoV communication delays," *IEEE Internet of Things J.*, vol. 9, no. 6, pp. 4090–4109, Mar. 2022, doi: 10.1109/JIOT.2021.3102841.

Yongfu Li (Senior Member, IEEE) received the Ph.D. degree in control science and engineering from Chongqing University, Chongqing, China, in 2012.

He is currently a Professor of control science and engineering with the Chongqing University of Posts and Telecommunications. His research interest focuses on connected and autonomous vehicles.

Qingxiu Lv is currently pursuing the M.S. degree in control engineering with the Chongqing University of Posts and Telecommunications, Chongqing.

His research interest covers platoon control of vehicles.

Hao Zhu (Member, IEEE) received the Ph.D. degree in computer science from Chongqing University, Chongqing, China, in 2012.

He is currently a Professor with the College of Automation, Chongqing University of Posts and Telecommunications, Chongqing. His research interests focus on intelligent vehicles and sensor fusion.

Haiqing Li (Associate Member, IEEE) received the Ph.D. degree in vehicle engineering from the Nanjing University of Aeronautics and Astronautics, China, in 2019.

He is currently a Lecturer at the Chongqing University of Posts and Telecommunications. His research interests include decision making of the connected and automated vehicles and vehicle dynamics control.

Huaqing Li (Senior Member, IEEE) received the Ph.D. degree in computer science and technology from Chongqing University in 2013.

He is currently a Professor at the College of Electronic and Information Engineering, Southwest University. His main research interests include nonlinear dynamics and control, multi-agent systems, and distributed optimization.

Simon Hu (Member, IEEE) received the Ph.D. degree in transport system engineering from Imperial College London in 2011.

He is currently an Assistant Professor at the Zhejiang University/University of Illinois at Urbana-Champaign Institute, Zhejiang University, China. His research interests lie in connected and autonomous vehicles and data fusion.

Shuyou Yu (Member, IEEE) received the Ph.D. degree in engineering cybernetics from the University of Stuttgart, Germany, in 2011.

He is currently a Full Professor with the Faculty of the Department of Control Science and Engineering, Jilin University, China. His current research interest focuses on predictive control.

Yibing Wang (Member, IEEE) received the Ph.D. degree in control theory and applications from Tsinghua University, Beijing, China, in 1998.

He is currently a Full Professor with the College of Civil Engineering and Architecture, Institute of Transportation Engineering, Zhejiang University, Hangzhou, China. His research interests include traffic flow modeling and vehicular *ad-hoc* networks.

Authorized licensed use limited to: Zhejiang Lab. Downloaded on May 06,2022 at 00:50:41 UTC from IEEE Xplore. Restrictions apply.